p38α MAPK signaling drives pharmacologically reversible brain and gastrointestinal phenotypes in the SERT Ala56 mouse

Matthew J. Robson[a,b], Meagan A. Quinlan[a,c], Kara Gross Margolis[d], Paula A. Gajewski-Kurdziel[a], Jeremy Veenstra-VanderWeele[e], Michael D. Gershon[f], D. Martin Watterson[g], and Randy D. Blakely[a,h,1]

[a]Department of Biomedical Science, Charles E. Schmidt College of Medicine, Florida Atlantic University, Jupiter, FL 33458; [b]Division of Pharmaceutical Sciences, University of Cincinnati, Cincinnati, OH 45220 [c]Department of Pharmacology, Vanderbilt University School of Medicine, Nashville, TN 37232; [d]Department of Pediatrics, Columbia University College of Physicians and Surgeons, New York, NY 10032; [e]Department of Psychiatry, Columbia University College of Physicians and Surgeons/New York Psychiatric Institute, New York, NY 10032; [f]Department of Pathology and Cell Biology, Columbia University College of Physicians and Surgeons, New York, NY 10032; [g]Department of Pharmacology, Northwestern University School of Medicine, Chicago, IL 60611; and [h]Brain Institute, Charles E. Schmidt College of Medicine, Florida Atlantic University, Jupiter, FL 33458

Edited by Susan G. Amara, National Institutes of Health, Bethesda, MD, and approved August 28, 2018 (received for review May 28, 2018)

Autism spectrum disorder (ASD) is a common neurobehavioral disorder with limited treatment options. Activation of p38 MAPK signaling networks has been identified in ASD, and p38 MAPK signaling elevates serotonin (5-HT) transporter (SERT) activity, effects mimicked by multiple, hyperfunctional SERT coding variants identified in ASD subjects. Mice expressing the most common of these variants (SERT Ala56) exhibit hyperserotonemia, a biomarker observed in ASD subjects, as well as p38 MAPK-dependent SERT hyperphosphorylation, elevated hippocampal 5-HT clearance, hypersensitivity of CNS 5-HT_{1A} and 5-$HT_{2A/2C}$ receptors, and behavioral and gastrointestinal perturbations reminiscent of ASD. As the α-isoform of p38 MAPK drives SERT activation, we tested the hypothesis that CNS-penetrant, α-isoform–specific p38 MAPK inhibitors might normalize SERT Ala56 phenotypes. Strikingly, 1-week treatment of adult SERT Ala56 mice with MW150, a selective p38α MAPK inhibitor, normalized hippocampal 5-HT clearance, CNS 5-HT_{1A} and 5-$HT_{2A/2C}$ receptor sensitivities, social interactions, and colonic motility. Conditional elimination of p38α MAPK in 5-HT neurons of SERT Ala56 mice restored 5-HT_{1A} and 5-$HT_{2A/2C}$ receptor sensitivities as well as social interactions, mirroring effects of MW150. Our findings support ongoing p38α MAPK activity as an important determinant of the physiological and behavioral perturbations of SERT Ala56 mice and, more broadly, supports consideration of p38α MAPK inhibition as a potential treatment for core and comorbid phenotypes present in ASD subjects.

serotonin | serotonin transporter | p38 MAPK | autism spectrum disorder

Autism spectrum disorder (ASD) is a common, male-predominant, neurodevelopment disorder with a significant and complex genetic risk architecture (1, 2), characterized by deficits in social communication/interaction and restricted and repetitive behavior (3). Recent estimates indicate a prevalence of ASD in the United States of 1 in 59 children, with a well-established 4:1 male predominance (4, 5). The economic burden on families for lifelong support of individuals with ASD is substantial, with individual costs for care in the United States estimated at $2.4 million (6), yielding a societal burden expected to exceed $400 billion annually by 2025 (7). Contributing to these costs are inadequate pharmacotherapies. Currently, there are only two Food and Drug Administration-approved medications for the treatment of ASD (aripiprazole and risperidone), neither of which ameliorate core symptoms of the disorder (8). Several recent advancements in the understanding of ASD mechanisms have spawned hope for the development of biologically grounded therapeutics (9, 10).

For over 50 y (11, 12), studies have found elevated whole-blood serotonin (5-HT) levels, termed hyperserotonemia, in a substantial subpopulation comprising 25–30% of children with ASD. Hyperserotonemia is unique to ASD, as opposed to other developmental disorders (13, 14), and blood 5-HT levels are highly heritable, as is ASD (15, 16). In the blood, 5-HT is contained almost entirely in platelets, which lack the ability to synthesize 5-H, acquiring the monoamine via a high-affinity, plasma membrane 5-HT transporter (SERT) (11, 12, 17). SERT is a Na^+/Cl^--dependent, high-affinity 5-HT transporter that, along with high expression in platelets, is also significantly expressed by neurons of the central and enteric nervous systems (CNS/ENS), subsets of endocrine cells (18), gastrointestinal epithelial cells, and placental synctiotrophoblasts (19), among other cells (20–22). SERT is antagonized by commonly prescribed antidepressants (23). Alterations in SERT expression and function have been linked to neuropsychiatric disorders, including depression, anxiety, obsessive-compulsive disorder, ASD (24, 25), as well as irritable bowel syndrome and inflammatory bowel disease (26). SERT is encoded by a single gene with no coding differences distinguishing CNS and peripheral transporters. The contribution

Significance

Autism spectrum disorder (ASD) is a neurodevelopmental disorder characterized by communication and social behavior deficits, repetitive behaviors, and medical comorbidities, including gastrointestinal dysfunction. No pharmacologic treatments are available that ameliorate core symptoms. Genetic variants in the serotonin transporter (SERT) are linked to ASD. Here we demonstrate that administration of a CNS-penetrant p38α MAPK antagonist normalizes multiple physiological and behavioral perturbations reminiscent of ASD in adult, SERT Ala56 mice. Conditional genetic manipulations validate a requirement for 5-HT neuron p38α MAPK signaling in establishing perturbations observed in SERT Ala56 mice. Our findings suggest that p38α MAPK may be a potential target for treatment of adults with ASD, particularly in relation to traits driven by elevated SERT activity and diminished 5-HT signaling.

Author contributions: M.J.R., J.V.-V., M.D.G., D.M.W., and R.D.B. designed research; M.J.R., M.A.Q., K.G.M., P.A.G.-K., M.D.G., and R.D.B. performed research; M.J.R., M.D.G., D.M.W., and R.D.B. contributed new reagents/analytic tools; M.J.R., M.A.Q., K.G.M., J.V.-V., M.D.G., D.M.W., and R.D.B. analyzed data; and M.J.R., J.V.-V., D.M.W., and R.D.B. wrote the paper.

Conflict of interest statement: J.V.-V. has served on advisory boards or consulted with Roche, Novartis, and SynapDx; has research funding from Roche, Novartis, SynapDx, Seaside Therapeutics, and Forest; and has also received editorial stipends from Springer and Wiley.

This article is a PNAS Direct Submission.

[1]To whom correspondence should be addressed. Email: rblakely@health.fau.edu.

This article contains supporting information online at www.pnas.org/lookup/suppl/doi:10.1073/pnas.1809137115/-/DCSupplemental.

Published online October 8, 2018.

made by SERT to the CNS and peripheral 5-HT uptake, however, is highly regulated posttranslationally, including the control of transporter surface trafficking and 5-HT affinity, each of which can arise from activation of endogenous receptors and signaling pathways that ultimately lead to changes in 5-HT uptake and clearance rates (27, 28).

In a search for polymorphisms that contribute to male-specific linkage to ASD on chromosome 17, we identified five rare SERT coding variants (24, 29). The most common of these variants, Gly56Ala, is present in ∼1% of individuals in the United States. In our study of multiplex pedigrees, the Ala56 variant was overtransmitted to ASD individuals and associated with ASD, with a specific enrichment of rigid-compulsive traits and sensory aversion (24). In lymphoblastoid cell lines (30), as well as transfected cells (31), each of the SERT variants identified, including Ala56, conferred elevated 5-HT transport activity. Kinetic analyses revealed that the elevated activity of SERT Ala56 derives from an increase in 5-HT affinity (31), mirroring a transporter state that arises transiently following acute p38 MAPK activation (32). In transfected cells, we found SERT Ala56 to be hyperphosphorylated via a p38 MAPK-dependent pathway (31) and have implicated immune-responsive p38 MAPK signaling in SERT activation, 5-HT clearance, and behavior (33, 34). Importantly, elevated expression of p38 MAPK signaling components has been reported in the brains of ASD subjects (35).

In vivo characterization of SERT Ala56 knockin mice (36) demonstrated multiple phenotypes reminiscent of ASD, including hyperserotonemia, repetitive behavior, and deficits in social interactions and communication (37, 38). Recently, these mice have been shown to exhibit deficits in multisensory integration (39), a deficit observed in ASD (40), and consistent with the association of SERT Ala56 with sensory abnormalities (24). Mirroring the common occurrence of constipation (41), which correlates with whole-blood 5-HT levels in ASD (42), SERT Ala56 mice demonstrate increased intestinal transit time due to ENS dysfunction, a phenotype prevented by in utero and postnatal treatment of animals with the 5-HT_4 agonist, prucalopride. These findings are consistent with the hyperactivity of SERT Ala56 in limiting access of 5-HT_4 receptors to their natural agonist (43). In the CNS, SERT Ala56 mice exhibit increased 5-HT clearance, as assessed by in vivo chronoamperometry. Consistent with these findings, 5-$HT_{2A/2C}$ and 5-HT_{1A} receptors demonstrate hypersensitivity to peripherally administered receptor agonists, suggesting compensatory receptor up-regulation as a consequence of limited 5-HT stimulation (37). As with cultured cells, adult SERT Ala56 mice exhibit elevated basal transporter phosphorylation, an effect normalized by ex vivo treatment of synaptosomal preparations with a p38 MAPK inhibitor (37). The latter findings suggested to us that some physiological or behavioral manifestations of SERT Ala56 hyperactivity may be reversible in adulthood.

With respect to reversal of SERT Ala56 traits through in vivo p38 MAPK inhibition, several challenges are readily apparent, foremost being the lack, until recently (44, 45), of CNS penetrant, isoform-selective p38 MAPK antagonists. Four genes (α, β, γ, δ) encode p38 MAPKs, each with a broad tissue distribution (46). Recently, we demonstrated that conditional elimination of p38α MAPK in serotonergic neurons eliminated the ability of peripheral lipopolysaccharide (LPS) to support SERT activation by peripherally administered LPS (33). We hypothesized, therefore, that an α-isoform–selective, small-molecule inhibitor might reduce CNS SERT Ala56 activity and potentially lead to phenotype reversal. Recently, Roy and coworkers (44, 47) reported the development of a potent, bioavailable and CNS penetrant, p38α MAPK-selective inhibitor, with rodent studies demonstrating suppression of both proinflammatory cytokine up-regulation and cognitive deficits in two distinct amyloid based Alzheimer's disease models (45, 48). Herein, we demonstrate the ability of pharmacologic inhibition of p38α MAPK to normalize phenotypic and physiologic traits in the SERT Ala56 mouse model, effects mirrored by the effects of conditional p38α MAPK elimination in 5-HT neurons. Our findings support ongoing p38α MAPK signaling as essential to the physiological and behavioral alterations observed in SERT Ala56 mice and warrant consideration of the pharmacological targeting of p38α MAPK signaling pathways as a strategy for a therapeutic intervention of adults with ASD.

Results

Repeated Administration of a Selective p38α MAPK Inhibitor Normalizes 5-HT Clearance in SERT Ala56 Mice. Previous in vitro and ex vivo studies have established the presence of a trafficking-independent, SERT stimulatory pathway downstream of p38 MAPK activation (28). Anisomycin (49, 50) or IL-1β (32, 34) triggers increased 5-HT uptake in cultured cells and mouse brain synaptosomes, an effect antagonized by nonselective p38 MAPK inhibitors, although siRNAs targeted to the α-isoform can block anisomycin-induced SERT activation. Consistent with a role of p38α MAPK in SERT regulation, two recently developed, selective p38α MAPK inhibitors (MW108 and MW150) antagonized anisomycin (10 min, 100 nM) stimulation of SERT in stably transfected SK-N-MC cells. As shown in *SI Appendix*, Fig. S1, both reagents effectively attenuated anisomycin-induced SERT activation.

To explore the role of p38α MAPK in sustaining the functional hyperactivity of SERT Ala56 in vivo, we injected adult mice with 5 mg/kg MW150 once per day (QD) for 1 wk before evaluating hippocampal clearance of exogenously applied 5-HT by high-speed chronoamperometry (51). As previously reported (37), saline-injected SERT Ala56 mice demonstrated significantly elevated basal 5-HT clearance rates compared with SERT Gly56 littermates (Fig. 1 *A* and *B*). In mice treated with MW150, however, this difference was eliminated, with SERT Ala56 clearance rates reduced to those displayed by SERT Gly56 animals. Neither the elevated SERT activity of SERT Ala56 mice nor the normalization of SERT Ala56 activity by MW150 can be explained by changes in SERT protein production, as revealed by SERT Western blots (Fig. 1 *C* and *D*). MW150 also did not alter CNS 5-HT levels (Fig. 1*E*) or 5-HT turnover (5-HIAA/5-HT ratio) (Fig. 1*F*), consistent with a selective contribution of p38α MAPK in 5-HT neurons to SERT-mediated 5-HT clearance, compared with 5-HT synthesis, storage, or release. A lack of genotype effects on CNS 5-HT homeostasis in the context of a model that exhibits hyperserotonemia likely reflects differential impact of SERT on the synthesis, vesicular release, clearance, and metabolism of 5-HT in the periphery versus the CNS. We also found no effects of MW150 on CNS tissue levels of dopamine or norepinephrine (*SI Appendix*, Fig. S2). Similarly, we detected no differences in total SERT protein production, monoamine levels, or 5-HT turnover in either SERT Gly56 or SERT Ala56 mice administered MW108 (10 mg/kg, QD for 1 wk) (*SI Appendix*, Fig. S3).

Ongoing p38α MAPK Activity Sustains Pharmacologically Reversible 5-HT Receptor Hypersensitivities. In prior studies (37), we found that SERT Ala56 mice, relative to littermate controls, display hypersensitivity of 5-HT_{1A} receptors in vivo, as reflected by increased 8-OH-DPAT–induced hypothermia. We hypothesize that these findings reflect an in vivo up-regulation of 5-HT_{1A} signaling that arises as a consequence of more limited 5-HT exposure in the context of the elevated 5-HT clearance. Whether this alteration is a compensatory response to lifelong elevated 5-HT clearance, or is a consequence of ongoing reductions in 5-HT availability is unclear. To address this issue, we treated mice as described above with either saline or 5 mg/kg MW150, once a day for a week. As shown in Fig. 2*A*, saline-injected SERT Ala56 mice demonstrated a significantly increased hypothermic response to 8-OH-DPAT, repeating our earlier observations. Whereas treatment of SERT Gly56 mice with MW150 did not modify 8-OH-DPAT body temperature responses, SERT Ala56 mice treated with MW150 resulted in a normalization of hypothermia induced by 8-OH-DPAT, statistically indistinguishable to that seen with SERT Gly56 animals.

To determine whether findings of reversibility of 5-HT_{1A} receptor signaling generalize to other 5-HT receptors, we assessed 1-(2, 5-dimethoxy-4-iodophenyl)-2-aminopropane (DOI)-induced

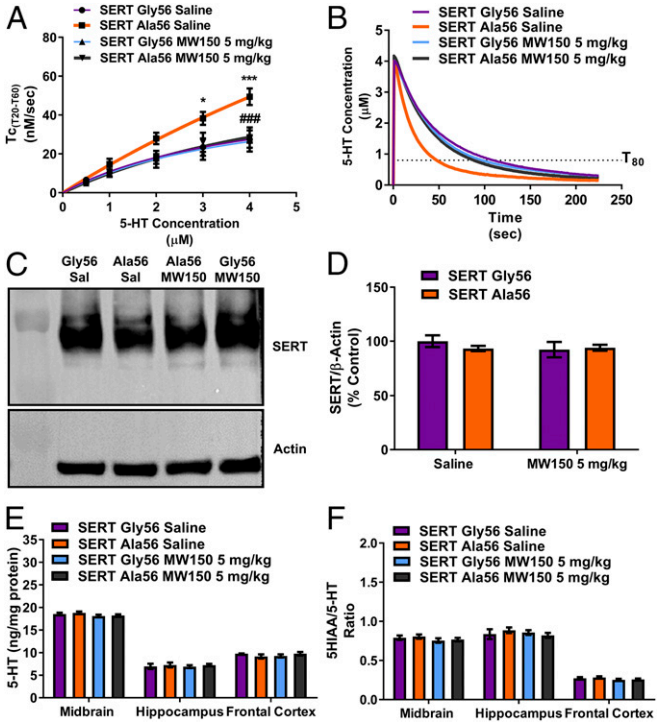

Fig. 1. Repeated p38α MAPK inhibitor administration normalizes hippocampal SERT activity in SERT Ala56 mice. (*A*) SERT Ala56 mice exhibit an elevated rate of hippocampal 5-HT clearance compared with their SERT Gly56 counterparts, an effect that is mitigated following repeated p38α MAPK inhibition with MW150 (5 mg/kg, i.p., QD × 7 d) (two-way repeated-measures ANOVA; main-effect group, $F_{3,\ 16} = 3.945$, $P = 0.02$; main-effect 5-HT concentration, $F_{4,\ 64} = 108.4$, $P < 0.001$, interaction of group by 5-HT concentration, $F_{12,\ 64} = 4.514$, $P < 0.0001$; $n = 5$ per group, followed by post hoc Bonferroni's multiple comparison tests, $^{*}P \leq 0.05$, $^{***}P \leq 0.001$ saline SERT Gly56 vs. saline Ala56; $^{\#\#\#}P \leq 0.001$ MW150 Ala56 vs. saline Ala56). (*B*) Grouped hippocampal 5-HT clearance curves for both SERT Gly56 and SERT Ala56 mice repeatedly administered either MW150 (5 mg/kg, i.p., QD × 7 d) or saline ($n = 5$ per group). (*C*) Unaltered total midbrain SERT expression postchronic p38α MAPK inhibition using MW150 (5 mg/kg, i.p., QD × 7 d) in SERT Gly56 or SERT Ala56 mice. (*D*) Quantified total SERT protein expression level as represented in *C* (two-way ANOVA treatment–genotype interaction $F_{1,\ 16} = 0.7898$, $P = 0.3873$, $n = 5$ per group, followed by post hoc Bonferroni's multiple comparison tests, n.s., not significant). (*E*) No differences in total 5-HT levels were detected after p38α MAPK inhibition in either SERT Gly56 or SERT Ala56 mice in the midbrain, hippocampus, or frontal cortex (two-way ANOVA interaction $F_{6,\ 71} = 0.6374$, $P = 0.6999$, followed by post hoc Tukey's multiple comparison tests, n.s., $n = 6$–9 per group.). (*F*) No alterations were detected in 5-HT turnover in the midbrain, hippocampus, or frontal cortex in SERT Gly56 or SERT Ala56 after p38α MAPK inhibition (two-way ANOVA interaction $F_{6,\ 71} = 0.2619$, $P = 0.6780$ $n = 6$–9 per group, followed by post hoc Tukey's multiple comparison tests, n.s.).

head-twitch responses in SERT Gly56 and SERT Ala56 mice, a behavior mediated by cortical 5-$HT_{2A/2C}$ receptors (52–54). Previously (37), we demonstrated that SERT Ala56 mice, relative to SERT Gly56 littermates, demonstrate an increase in head-twitch responses, findings we replicated in the present study using saline-injected cohorts (Fig. 2*B*). As observed with 8-OH-DPAT–induced hypothermic responses, head-twitch responses to DOI in SERT Ala56 mice were normalized by administration of MW150 once a day for a week (Fig. 2*B*). Corroborating the involvement of selective p38α MAPK inhibition in normalizing 5-$HT_{2A/2C}$ receptor sensitivity in SERT Ala56 mice, MW108 was found to dose-dependently normalize head-twitch responses to DOI in a similar fashion as MW150 administration (*SI Appendix*, Fig. S4*B*). Together with our findings of a normalization of 5-HT_{1A} responses, these results support a role for ongoing p38α MAPK-driven SERT Ala56 hyperactivity in mutation-induced modulation of 5-HT signaling pathways.

Ongoing p38α MAPK Activity Supports Social Interaction Deficits in SERT Ala56 Mice. SERT Ala56 mice display perturbations of normal social behavior, assessed in the three-chamber test of social interactions and in the tube test (37). Because the 129S4/S6 background on which the SERT Ala56 mice and their SERT Gly56 littermates are maintained imposes a general, SERT-independent reduction in spontaneous locomotor activity, making reversal studies in the three-chamber test inherently variable, we tested the effects of p38α MAPK inhibition on SERT Ala56-mediated social interaction deficits using the tube test. Consistent with our prior tube-test studies, vehicle-treated, adult SERT Ala56 knockin mice withdrew from an encounter with SERT Gly56 animals of the same genetic background (noted as "reduced wins") at levels significantly greater than expected (Fig. 2*C*). Once-a-day treatment with 5 mg/kg MW150 for 1 wk resulted in tube-test performance of SERT Ala56 mice equivalent to that of SERT Gly56 littermates. Similarly, once-a-day administration of MW108 was found to dose-dependently normalize SERT Ala56-mediated social interaction deficits (*SI Appendix*, Fig. S4*C*). These findings reveal that the reversibility of SERT Ala56 phenotypes extends beyond hypersensitivity of 5-HT receptors and encompasses complex behaviors initiated

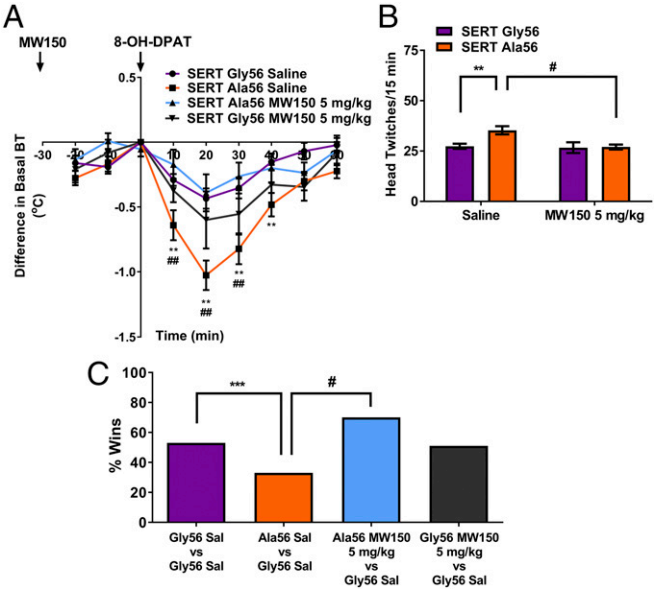

Fig. 2. Repeated administration of a p38α MAPK inhibitor reverses SERT Ala56-mediated 5-HT receptor hypersensitivities and social interaction deficits. (*A*) Repeated MW150 administration normalizes SERT Ala56-mediated 5-HT_{1A} receptor hypersensitivity (two-way repeated-measures ANOVA, interaction $F_{24,\ 472} = 3.757$, $P < 0.0001$, followed by post hoc Bonferroni's multiple comparison tests, $^{**}P \leq 0.01$ saline SERT Gly56 vs. saline SERT Ala56, $^{\#\#}P \leq 0.01$ MW150 SERT Ala56 vs. saline SERT Ala56, n = 7–23 per group.). Chronic MW150 administration was found to not exert any effects on basal body temperature or on 8-OH-DPAT–induced hypothermia in SERT Gly56 animals. (*B*) Repeated MW150 administration normalizes SERT Ala56-mediated 5-$HT_{2A/2C}$ hypersensitivity (two-way ANOVA interaction $F_{2,\ 54} = 6.568$, $P = 0.0028$, followed by post hoc Bonferroni's multiple comparison tests, $^{**}P \leq 0.01$ saline SERT Gly56 vs. saline SERT Ala56, $^{\#}P \leq 0.05$ SERT Ala56 MW150 vs. saline SERT Ala56, $n = 6$–13 per group). Repeated MW150 administration was found to not exert any effects on DOI-induced head-twitch behavior in SERT Gly56 animals. (*C*) Repeated MW150 administration reverses SERT Ala56-mediated social interaction deficits detected using the tube test (χ^2 with Yates correction, n = 37–97 bouts per group and $^{***}P \leq 0.001$, saline SERT Gly56 vs. saline Ala56, $^{\#}P \leq 0.05$, saline Ala56 vs. MW150 Ala56). Repeated MW150 administration exerted no effects alone in SERT Gly56 mice in the tube test.

PHARMACOLOGY

through social interactions, and further documents a role for ongoing p38α MAPK activity in SERT Ala56 phenotypes.

Repeated Administration of MW150 Is Required for Pharmacological Efficacy in Adult SERT Ala56 Mice. To ascertain whether acute inhibition of p38α MAPK results in the normalization of perturbations evident in the SERT Ala56 mice, these animals and their SERT Gly56 counterparts were treated with saline or 5 mg/kg MW150, intraperitoneally, 30 min before evaluation of DOI-induced head-twitch and tube-test behavior. We found that a single, acute administration of MW150 was without effect on 5-$HT_{2A/2C}$ receptor hypersensitivity evident in SERT Ala56 mice (*SI Appendix*, Fig. S5*A*). Acute inhibition of p38α MAPK also lacked the effects seen after 1-wk exposure for social interaction changes as assessed in the tube test (*SI Appendix*, Fig. S5*B*). These results indicate that the physiological and behavioral impact of p38α MAPK inhibition we describe with the SERT Ala56 model does not occur immediately, but rather arises from time-dependent changes in 5-HT signaling and neuromodulation.

Gastrointestinal Dysfunction in Adult SERT Ala56 Mice Relies on p38α MAPK Activity. Gastrointestinal (GI) dysfunction is a common medical comorbidity of ASD (55, 56). The presence of SERT and multiple 5-HT receptors in neurons, epithelial cells, and endocrine cells in the gut, and the GI disturbances that accompany genetic elimination of 5-HT biosynthesis, SERT, and GI 5-HT receptors (57), suggested to us that the SERT Ala56 model might display structural and functional GI abnormalities, adding further evidence for these mice as a face-valid model of ASD. Indeed, our prior studies revealed that SERT Ala56 mice demonstrate multiple gut abnormalities, including an enteric hypoennervation, diminished density of late-born enteric neuronal subsets, altered epithelial structure, and functional bowel deficits in motility (19). These changes were prevented when SERT Ala56 mice were exposed in utero and until weaning to the 5-HT_4 receptor agonist prucalopride, a receptor critical to proper ENS development. These findings are consistent with hyperfunction of SERT Ala56 limiting access of GI 5-HT_4 receptors to 5-HT during development, with the agonist able to replace the action of native 5-HT. As such, we expected MW150 would lack efficacy in reversing the GI abnormalities of SERT Ala56 mice when treatments were administered to adult animals. Surprisingly, ex vivo assessment of colonic motility suggests that this is not entirely true. Using isolated preparations of colon, we initiated colonic migrating motor complexes (CMMCs) by increasing the intraluminal pressure of these preparations as described in *Methods*. Video analysis revealed spatiotemporal maps of contractile activity patterns (Fig. 3*A*) that with SERT Ala56 preparations demonstrated reductions in CMMC frequency (Fig. 3*B*) and velocity (Fig. 3*C*) relative to SERT Gly56 preparations, similar to our previous reports (19). Remarkably, we found that 1-wk administration of MW150 at the same dose used for behavioral and CNS 5-HT clearance/pharmacology studies resulted in the normalization of SERT Ala56 deficits in both parameters (Fig. 3 *B* and *C*). Administration of MW150 induced an unexpected reduction in CMMC frequency in SERT Gly56 mice, the opposite effect of that seen with SERT Ala56 preparations, suggesting contributions of basal p38α MAPK signaling that may be lost with lifelong SERT Ala56 expression. Regardless, these effects point to an active, ongoing role of p38α MAPK signaling in maintaining normal, physiologic CMMC contributions to gut motility.

Genetic Evidence That p38α MAPK Expression in 5-HT Neurons Drives Phenotypes in SERT Ala56 Mice. Although we found that systemic treatment of SERT Ala56 animals with MW150 can rescue multiple biochemical, physiologic, and behavioral phenotypes, including ones reminiscent of either core or comorbid traits of ASD, we cannot conclusively link p38α MAPK to these phenotypes through pharmacological strategies alone, because of the inherent limits to understanding the full spectrum of a drug's action. Our prior studies demonstrating p38 MAPK-dependent hyper-

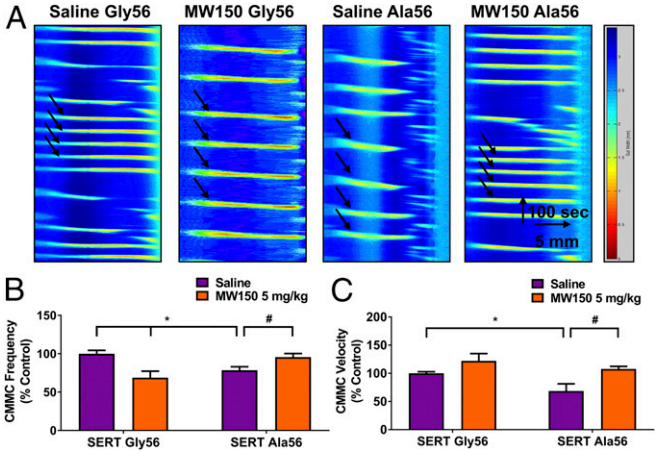

Fig. 3. Repeated administration of a p38α MAPK inhibitor reverses SERT Ala56-mediated reductions in intestinal motility. (*A*) Representative spatiotemporal maps showing CMMCs (highlighted by black arrows) in isolated colonic preparations from SERT Gly56 and SERT Ala56 mice administered either saline or MW150 (5 mg/kg, i.p., QD × 7 d). Ordinate axis represents time and the abscissa represents the distance from oral end to anal end of the resected colon. The width of the gut (millimeters) is pseudo-colored and indicative of contractions. (*B*) SERT Ala56-mediated reductions in CMMC frequency are normalized by MW150 administration. Data normalized to control (saline SERT Gly56) (n = 8–12 per group, two-way ANOVA, followed by post hoc Fisher's LSD multiple comparison tests, $F_{1,\ 60} = 17.12$, $^{*}P \leq 0.01$, saline SERT Gly56 vs. saline SERT Ala56 and saline SERT Gly56 vs. MW150 SERT Gly56, $^{\#}P \leq 0.05$ MW150 SERT Ala56 vs. saline SERT Ala56). (*C*) SERT Ala56-mediated reductions in CMMC velocity are normalized by MW150 administration. Data normalized to control (saline SERT Gly56) (n = 8–12 per group, two-way ANOVA, followed by post hoc Fisher's least-significant difference multiple comparison tests, $F_{1,\ 60} = 10.47$ and 14.19, $^{*}P \leq 0.05$, saline SERT Gly56 vs. saline SERT Ala56, $^{\#}P \leq 0.05$ MW150 SERT Ala56 vs. saline SERT Ala56).

phosphorylation of SERT Ala56 in both transfected cells (31) and in nerve terminal preparations (37) suggests that the requisite site of p38α MAPK inhibition may be within serotonergic neurons. Because SERT is also expressed by nonneuronal cells (22, 58–62), our hypothesis cannot be tested using only systemic drug studies. To validate the specific site of MW150 action and determine whether 5-HT neuron p38α MAPK supports SERT Ala56 phenotypes, we implemented a conditional gene-targeting strategy, whereby the SERT Ala56 variant is expressed in mice with a 5-HT neuron-specific elimination of p38α MAPK. In prior studies, we established that 5-HT neuron-specific elimination of p38α MAPK, achieved by expressing Cre in p38α $MAPK^{loxP/loxP}$ mice under the control of the *Pet-1* promoter (63, 64), could prevent SERT stimulation and depression-like behavior following a peripheral LPS injection (33). Here, we crossed the SERT Ala56 allele onto a p38α $MAPK^{loxP/loxP}$:ePet1::Cre background and then bred animals to generate p38α $MAPK^{loxP/loxP}$:SERT Ala56 (Ala56 p38α^{5HT+}) and p38α $MAPK^{loxP/loxP}$:ePet1::Cre:SERT Ala56 (Ala56 p38α^{5HT-}) littermates. With these mice, we tested for 5-HT_{1A} and 5-$HT_{2A/2C}$ sensitivity and social function, as described above.

Similar to our previous reports utilizing p38α $MAPK^{loxP/loxP}$:ePet1::Cre mice (33), we observed a marked reduction of p38α MAPK immunoreactivity in 5-HT neurons of Ala56 p38α^{5HT-} mice compared with their Ala56 p38α^{5HT+} littermates (Fig. 4). Utilizing the in vivo 8-OH-DPAT–induced hypothermia assay, we found that Ala56 p38α^{5HT-} mice displayed a significant reduction in 5-HT_{1A} receptor sensitivity, compared with their Ala56 p38α^{5HT+} littermates (Fig. 5*A*). Similarly, Ala56 p38α^{5HT-} mice exhibited a significantly reduced sensitivity to 5-$HT_{2A/2C}$ receptor stimulation in the DOI-induced head-twitch assay (Fig. 5*B*) compared with Ala56 p38α^{5HT+} controls. Finally, Ala56 p38α^{5HT-} mice demonstrated increased "wins" in the tube

test, whether using SERT Gly56 animals for comparison (Fig. 5*C*), or when tested against Ala56 p38α^{5HT+} animals (Fig. 5*D*). These studies provide genetic evidence in support of p38α MAPK activity in 5-HT neurons as a major, ongoing determinant of receptor and behavioral changes arising in SERT Ala56 mice.

Discussion

Therapeutics that ameliorate the core symptoms of ASD remain unavailable and, with the increasingly recognized high prevalence of the disorder (5), are sorely needed. Although we recognize that complex behavioral disorders like ASD are only incompletely modeled in animals, these constructs provide key opportunities to test hypotheses related to brain alterations that may drive ASD risk and novel therapeutic leads. The identification of rare, disease-associated genetic variation that lies within protein-coding regions provides an opportunity to build such models following validation of functional effects in vitro. We identified the SERT Ala56 substitution, along with four other SERT coding variants, in a multiplex ASD population (24, 29). Remarkably, we found each variant to confer elevated 5-HT uptake using transfected cells, compared with cells transfected with WT SERT Gly56. In this multiplex population, SERT Ala56 was overtransmitted to affected subjects who were enriched for rigid-compulsive traits and sensory aversion (24). In our knockin mice, SERT Ala56 produces readily discernible serotonergic system dysfunction and behavioral changes (36, 37, 43). SERT Ala56 mice also exhibit a p38 MAPK-induced elevation in SERT phosphorylation (37), consistent with p38 MAPK signaling as a critical determinant of SERT Ala56 hyperactivity (27, 50, 65). Recently, we demonstrated that both pharmacologic inhibition and genetic elimination of p38α MAPK in 5-HT neurons can normalize elevated SERT activity, as well as despair-like behaviors, which arise following acute innate immune system activation (33, 34).

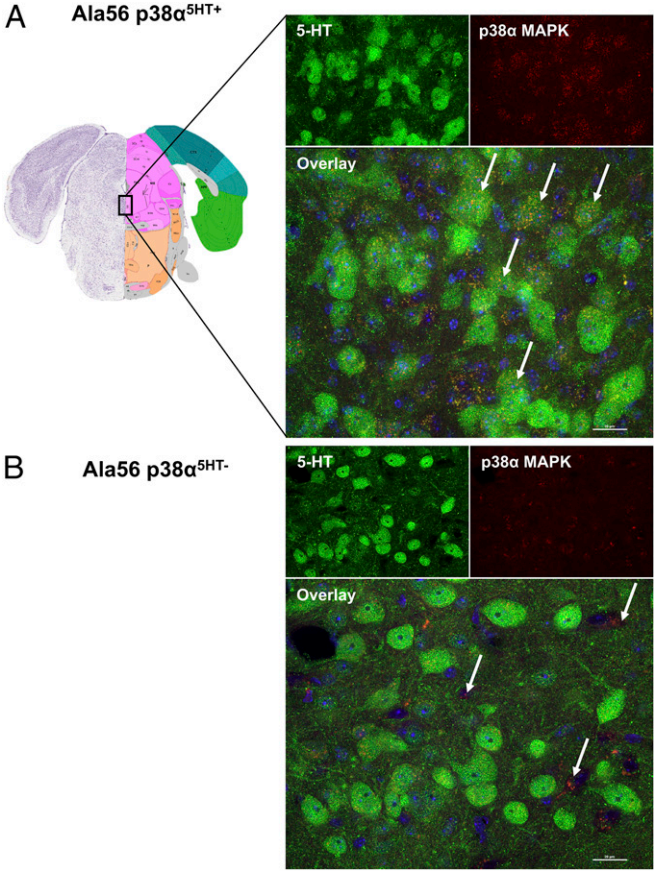

Fig. 4. Immunohistological characterization of p38α MAPK elimination in 5-HT neurons of SERT Ala56 mice in the dorsal raphe utilizing Cre recombinase expression driven by *pet-1*. (*A*) Expression of p38α MAPK in 5-HT neurons of p38α MAPK$^{loxP/loxP}$:SERT Ala56$^{+/+}$ (Ala56 p38α^{5HT+}) mice. White arrows denote the presence of p38α MAPK in 5-HT neurons of the dorsal raphe. (*B*) Reduction of expression specifically within 5-HT neurons within the dorsal raphe of p38α MAPK in p38α MAPK$^{loxP/loxP}$:ePet1::Cre:SERT Ala56$^{+/+}$ (Ala56 p38α^{5HT-}) mice. White arrows in *B* denote p38α MAPK immunoreactivity in various cell types of the raphe nucleus other than 5-HT neurons in Ala56 p38α^{5HT-} mice. Images = 60×. (Scale bar, 20 μM.)

In the present study, we sought to determine whether p38α MAPK signaling underlies phenotypes observed in the SERT Ala56 knockin mouse. We initially implemented a pharmacological approach, using two CNS penetrant and isoform-selective p38α MAPK inhibitors, MW108 and MW150. Following initial positive findings with MW108 (data in figures in *SI Appendix*), a MW108 analog with improved drug development potential and comparable potency/selectivity for p38α MAPK inhibition, MW150, became available. Our report therefore focuses on the use of this reagent to ascertain the role of p38α MAPK in SERT Ala56 phenotypes. Indeed, we observed a normalization of elevated 5-HT clearance after daily, repeated administration of MW150 to adult mice, and a remarkable ability of the drug to reverse multiple physiological and behavioral phenotypes. We obtained evidence that supports the specificity of MW150 (and MW108) for p38α MAPK through genetic elimination of the enzyme, and gained further evidence for a cell-autonomous role of p38α MAPK by selectively eliminating the kinase in 5-HT neurons, where we also observed normalization of 5-HT receptor hypersensitivity and social interaction deficits. Trait normalization by MW150 in adult SERT Ala56 mice was not immediate, but required repeated administration of the drug. The lack of efficacy of acute MW150 administration suggests a time-delay between a normalization of synaptic 5-HT availability and the molecular, cellular, or circuit adaptations that drive physiological and behavioral responses under serotonergic control. Possible time-dependent mechanisms include change in 5-HT neuron firing arising from changes in 5-HT$_{1A}$ receptor signaling, alterations in the expression of postsynaptic 5-HT receptors, or circuit-based adaptations that require gene induction and the synthesis of key signal transduction machinery. A greater understanding of the temporal requirement for p38α MAPK inhibition may reveal additional targets for therapeutic development, particularly as it relates to ASD risk impacted by changes in 5-HT signaling. More remarkable is that treatment of adult animals with MW150 produced trait normalization. We acknowledge that the assays employed in our study sample only a small proportion of likely deficits exhibited in the model, and that the impact of elevated 5-HT clearance on brain development may establish traits that do not respond to p38α MAPK inhibition. It is also possible that the hyperactivity of SERT Ala56 is absent early in development due to contextual factors that limit the actions of p38α MAPK.

We found that the inhibition of p38α MAPK normalizes social-interaction behavior in the tube test, an assay predominantly used to probe social hierarchies and dominance (66, 67). In the present report, SERT Ala56 mice and their SERT Gly56 counterparts were paired off against noncage-mates, whereas classically the assay is conducted with cage-mate pairings to assess dominance relationships established via a preestablished social hierarchy (66). In our version of the tube test, we probe initial, albeit forced social interactions between two animals that have never encountered one another, precluding establishment of such hierarchies. We hypothesize that conducting the assay in this manner queries aspects of social interaction independent of dominance-driven aggression behaviors. Consistent with this idea, a recent report indicates that tube-test behavior correlates with social motivation, as assessed in the Crawley three-chamber sociability task, although more work is clearly needed in this area (67). It should be noted that the SERT Ala56 mice also exhibit social deficits in the

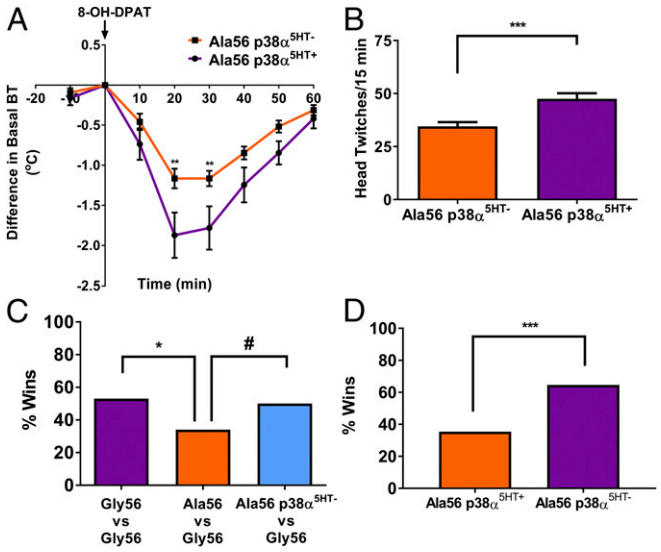

Fig. 5. Conditional genetic elimination of p38α MAPK in 5-HT neurons reverses SERT Ala56-mediated 5-HT receptor hypersensitivity and social interaction deficits. (*A*) Conditional elimination of p38α MAPK in Ala56 p38α^{5HT-} mice results in a significant reduction in 5-HT$_{1A}$ receptor sensitivity as assessed by an in vivo 8-OH-DPAT hypothermia assay (two-way ANOVA interaction $F_{7,\ 182} = 3.538$, $P = 0.0014$, $^{**}P \leq 0.01$ Ala56 p38α^{5HT-} vs. Ala56 p38α^{5HT+}, $n =$ 11–17 per group.). (*B*) Ala56 p38α^{5HT-} mice exhibit significantly reduced 5-HT$_{2A}$ receptor sensitivity compared with their Ala56 p38α^{5HT+} counterparts as assessed using an in vivo DOI-induced head-twitch assay (unpaired t test, $^{***}P = 0.0007$, $t = 3.974$, $n = 9$–12 per group). (*C*) Ala56 p38α^{5HT-} mice exhibit a reversal of social interaction deficits present in SERT Ala56 mice compared with SERT Gly56 animals (χ^2 with Yates correction, $n = 74$–121 bouts per group, $^{*}P \leq 0.05$ SERT Gly56 vs. Ala56, $^{\#}P \leq 0.05$ Ala56 vs. Ala56 p38α^{5HT-}). (*D*) Conditional elimination of p38α MAPK in 5-HT neurons of SERT Ala56 mice (Ala56 p38α^{5HT-}) results in a larger number of wins in the tube test compared with their Ala56 p38α^{5HT+} counterparts (χ^2 with Yates correction, $n = 127$ bouts/group, $^{***}P \leq 0.001$ Ala56 p38α^{5HT-} vs. Ala56 p38α^{5HT+}).

Crawley three-chamber analysis (37). However, because of inadequate levels of spontaneous locomotor activity in the SERT Ala56 line (37), attempts at pharmacologic reversal in this assay using this particular genetic line are problematic. Moreover, we were encouraged to pursue the tube test to query social interactions due to reports of deficits in this test using Fmr1$^{-/-}$ mice (68), animals expressing the most common genetic cause of ASD.

Alterations in 5-HT homeostasis and signaling have been reported in ASD for many years (69–72), beginning with the studies of Schain and Freedman (12) who first described hyperserotonemia as a quantitative trait associated with ASD. Besides subsequent replications of hyperserotomia (11, 13, 17), early positron emission tomography (PET) studies of CNS 5-HT turnover found differences between ASD subjects and typically developing individuals (72–74). Association studies have implicated variation in the SERT gene (*SLC6A4*), as well as the SERT-associated protein integrin subunit β-3 gene (*ITGB3*) in establishing both blood 5-HT levels and ASD risk (37, 75–79). Additionally, dietary depletion of tryptophan, the essential amino acid precursor of 5-HT, has been reported to worsen symptoms in ASD subjects (80), an effect recapitulated in rodent models (81), suggesting that a reduction in 5-HT availability for signaling could sustain ASD traits. Despite these findings, 5-HT selective reuptake inhibitors (SSRIs), which elevate extracellular 5-HT, have shown no significant benefit for ASD symptoms in randomized trials, with frequent adverse events in children with ASD, including irritability and insomnia (82, 83). In contrast, some benefit has been reported for SSRIs in adults with ASD (84, 85). Overall, these findings yield a complex picture for SSRIs in ASD, with poor tolerability in children and an unclear pattern of symptom response. Our work suggests that evaluating ASD therapies, including SSRIs, in subjects with hyperserotonemia may be of value. Importantly, our findings suggest that enhancing 5-HT signaling through p38α MAPK inhibition may provide a more subtle and effective therapy than direct SERT antagonism.

Other ASD-related models show abnormalities in 5-HT signaling, suggesting a broader relevance for our findings. As noted above, the most common genetic disruption that gives rise to ASD traits arises at the *Fmr1* locus in fragile X syndrome (FXS). Physiologic and behavioral traits of Fmr1$^{-/-}$ mice can be normalized or exacerbated via pharmacological manipulation of 5-HT signaling (86–88), aligning with some findings in humans with FXS (89–91). Additionally, transgenic mice bearing an ASD-associated 15q11-13 duplication (*15q dup* mice) exhibit alterations in dorsal raphe 5-HT synaptic transmission, with concomitant changes in midbrain 5-HT and 5HIAA levels and social behavior and vocalization deficits (92), deficits rescued by early-life administration of the SRI fluoxetine (92). The heightened sensitivity of 5-HT$_{2A}$ receptors we have reported in SERT Ala56 animals has also been observed in other genetic and environmental murine models for ASD. As in our model, mice expressing the ASD-associated 16p11.2 deletion exhibit increased head-twitch responses to DOI (93). Moreover, Walsh et al. (94) have provided compelling evidence for diminished 5-HT signaling in the nucleus accumbens in this model that drives sociability deficits. 5-HT$_{2A}$ receptor functionality has been linked to reversal learning deficits in BTBR *T*$^{+}$*Tf*/*J* mice (95), an inbred line that exhibits profound social behavior deficits (96–98). The BTBR *T*$^{+}$*Tf*/*J* model has multiple abnormalities in the 5-HT system (99); moreover, antagonizing BTBR *T*$^{+}$*Tf*/*J* 5-HT$_{2A}$ receptor function reverses these deficits (95) and reduces excessive grooming behavior (100). Maternal infection with the viral-mimetic Poly I:C (MIA, a commonly utilized model for environmental triggers of ASD) has been shown to result in adult offspring with increased sensitivity to DOI, an effect that correlated to increased expression of 5-HT$_{2A}$ receptors within the prefrontal cortex (101). An examination of the ability of MW150 and serotonergic p38α MAPK deletion to normalize physiological and behavioral traits in these models should be explored in future studies.

Although the diagnostic features of ASD are behavioral in nature, medical comorbidities are common, including constipation, which is associated with whole-blood 5-HT levels (42, 102, 103). Functional differences in the GI tract of ASD probands is associated with rigid-compulsive behavior (104), clinical deficits that mirror the functional and behavioral deficits exhibited in SERT Ala56 mice (37, 43). We have previously shown that SERT Ala56 mice exhibit deficits in ENS development as well as colonic motility (43), effects that can be prevented by 5-HT$_4$ receptor activation during development. In the present study, we demonstrate that MW150 in adulthood normalizes CMMC frequency and velocity, representative of a restoration of the function of intrinsic ENS circuitry. Surprisingly, we found that colonic segments isolated from SERT Gly56 mice administered MW150 demonstrated a reduction in CMMC frequency, whereas this parameter is normalized in preparations obtained from their SERT Ala56 counterparts. These findings indicate the presence of a basal, positive contribution made by p38α MAPK activity to CMMC generation in SERT Gly56 animals, a contribution lost in SERT Ala56 mice, presumably arising from the aforementioned developmental effects of SERT Ala56 expression, whereas the normalization effect of MW150 demonstrates a second, ongoing contribution sensitivity of p38α MAPK, consistent with expectations from CNS and behavior studies.

Our ability to reverse colonic function through adult administration of MW150 was surprising, given the significant changes in enteric neuron development that arise in SERT Ala56 mice. Because 5-HT is a well-recognized promotor of GI motility (105, 106), the normalization of colonic function in SERT Ala56 mice by MW150 may derive from a potentiation of 5-HT action at enteric synapses, overcoming developmental abnormalities. It is also possible that p38α MAPK inhibition influences bowel function through 5-HT–dependent increases in enteric neurogenesis, which continues in the ENS into adulthood (43, 107,

108). Finally, constitutive expression of SERT Ala56 may drive inflammation in the gut, with an alleviation of symptoms arising from reductions in inflammatory cytokine signaling elicited by the inhibition of p38α MAPK. Future studies should address whether the beneficial effects of MW150 arise in the SERT Ala56 model from a functional potentiation of 5-HT signaling or more indirectly, such as through gut- or microbiome-modulated inflammatory signaling that intersects with gut 5-HT mechanisms. Regardless, p38α MAPK inhibition represents a potentially useful strategy for relief of GI distress in ASD, possibly of greatest benefit to subjects with other indications of altered 5-HT function, such as hyperserotonemia.

Activation of p38α MAPK can arise from a myriad of physiologic and environmental factors, including heat stress, inflammation, and the actions of proinflammatory cytokines, UV light, and reactive oxygen and reactive nitrogen species (46, 109). Additionally, activation of the α-isoform of p38 MAPK is involved in innate immune responses to these stimuli (46), an effect that we have previously linked to increased CNS SERT clearance (32, 34). Aberrations in immune system function have repeatedly been detected in ASD cohorts (110, 111) (including increases in IL-1β, a proinflammatory cytokine which activates p38 MAPK signaling) (112), and in various environmental and genetic rodent models for ASD (113–115). Furthermore, postmortem genetic analysis in ASD cohorts has revealed altered p38 MAPK signaling (35). Models for environmentally induced ASD, such as mice subjected to MIA, have revealed long-lasting immune system dysregulation and behavioral changes reminiscent of the disorder (114, 116, 117). Combined, these studies suggest a convergence of p38 MAPK-dependent inflammatory signaling mechanisms and 5-HT–dependent pathways in ASD that may represent a promising target for ASD pharmacotherapy development.

Based on previous studies, as well as our present results, p38α MAPK is emerging as a neurotherapeutic target in a diverse array of neurologic disorders, particularly where origins appear to stem from an intersection of neuronal and inflammatory signaling (44, 45, 118). MW150 is a highly selective, CNS-penetrant, orally bioavailable drug candidate with a unique set of pharmacological features that removes previous barriers to the clinical development of p38α MAPK inhibitors (45, 119). Prior studies have revealed utility of this class of molecules for ameliorating the effects of genetic and environmental insults imposed to model neurodegenerative disorders, including stroke and Alzheimer's disease (45, 119, 120). Our work extends the potential utility of p38α MAPK inhibitors for the treatment of a prevalent behavioral disorder, one where effective pharmacotherapies are limited.

Methods

MW108 and MW150 Generation and Administration. MW150 and MW108 were synthesized and characterized as previously described (44, 119). Both MW108 and MW150 were tested for kinome selectivity using single blinded studies designed to detect cross-over to other kinome members, detectable to a level of approximate 0.5% sensitivity (44, 119). Similarly, cross-over to major G protein-coupled receptor classes were done via cell-based functional screens for agonist or antagonist function. Dose-dependent efficacy, target engagement, and pharmacodynamic effects, as well as high-dose range-finding safety studies with associated toxicokinetics and observational and histological analyses were also performed. Although both MW108 and MW150 have comparable CNS penetrance (B/P ratio $\geq$ 0.9) and isoform selectivity, we focused the majority of our in vivo efforts on MW150 due to its superior metabolic stability and bioavailability (44, 119). All p38α MAPK inhibitor treatments were conducted utilizing drug dissolved in sterile saline (Hospira) in sterile vials (Thermo Scientific) and used at 0.1 mL/10 g body weight for all doses. Vehicle treatments were conducted using sterile saline injections (0.1 mL/10 g body weight, intraperitoneally). Repeated administration regimens of p38α MAPK inhibitors consisted of intraperitoneal, QD for 7 d before undergoing behavioral or biochemical analyses. Dosing regimens were selected based upon previous reports of p38α MAPK inhibition utilizing MW150 in vivo (45, 121). Single administration dosing consisted of an intraperitoneal injection or either MW150 or vehicle (sterile saline) 30 min before commencement of behavioral/biochemical assay. Additional time windows for single administration effects were not conducted as part of this investigation.

Animals. Mice on a 129S6/S4 background that are homozygous for sequences encoding SERT Gly56 (WT) or SERT Ala56 proteins were used to test drug and genetic manipulation of p38α MAPK. Littermates homozygous for either variant were obtained from heterozygous dams and sires. All data from animals were derived from multiple cohorts that were bred and analyzed under a protocol annually reviewed by the Institutional Animal Care and Use Committees of Vanderbilt University or Florida Atlantic University. Animals were housed on a 12:12 light:dark cycle and tested during the light phase. Food was provided ad libitum. All studies were performed with male animals because of the 4:1 male bias observed with ASD, the male-specific linkage region that harbors the *SLC6A4* gene encoding SERT, and the preponderance of published data demonstrating trait differences in male, SERT Ala56 mice.

Behavioral Analyses. All behavioral experiments were conducted in the Vanderbilt University or Florida Atlantic University Murine Behavior Core using mice that were transferred to the facility between the ages of 5 and 8 wk of age. All mice were between 8 and 16 wk of age at time of testing. All experiments were conducted after at least a 7-d acclimation period. Each experiment was conducted after at least a 30-min acclimation period to the specific testing facility.

Tube Test. The tube test was conducted as previously described (37). Male SERT Ala56 mice and their SERT Gly56 littermates were administered either vehicle (saline, 0.1 mL/10 g body weight, intraperitoneally, repeatedly or acutely administered) MW108 (5–10 mg/kg, i.p.) or MW150 (5–10 mg/kg, i.p, repeatedly or acutely administered). Animals were trained for 2 d before the testing day. Training days consisted of running the mice through the tube apparatus that consists of a 30-cm-long, 3.5-cm-diameter clear acrylic tube with small, acrylic funnels attached to each end to aid in entry into the tube. Progress completely through the tube in both directions on training days resulted in the mice being placed back into their respective home cages. Mice that did not initially enter the tube were encouraged to run forward with a gentle pull of the tail. On testing day, pairings were run in both directions as previously described to avoid positional bias and were paired off against all counterparts present in the opposing home cage (37, 68). For each testing bout, randomized mice from the same sex and age cohorts but separate and distinct home cages were placed at the opposite ends of the tube and released. Each subject was declared a "winner" when their respective opponent backed out of the tube. If neither animal backed out of the tube after a time period of 2 min, a draw was declared. Draws were excluded from analysis. All wins and losses were included in analysis of tube-test data.

DOI-Induced Head Twitch. DOI-induced head twitch was conducted as previously described (37). Briefly, male SERT Ala56 mice and their SERT Gly56 littermates treated with either vehicle (saline, 0.1 mL/10 g body weight, intraperitoneally, repeatedly or acutely administered) MW108 (5–10 mg/kg, i.p.) or MW150 (5–10 mg/kg, i.p, repeatedly or acutely administered) underwent treatments of DOI (1.0 mg/kg, i.p.; Sigma Aldrich) dissolved in sterile saline (0.1 mL/10 g body weight). Thirty-four minutes posttreatment, each respective mouse was placed in a large glass beaker (4 L) containing bedding (1 cm) and two independent reviewers blinded to genotype independently counted head twitches over a period of 15 min. Head twitches were quantified and analyzed.

8-OH-DPAT–Induced Hypothermia. 5-HT_{1A} receptor sensitivity was assessed utilizing treatments of 8-OH-DPAT, as previously described (37). Thirty minutes before treatment with 8-OH-DPAT (Sigma Aldrich), mice underwent their final administration of either vehicle (saline), MW108, or MW150 as described above. Following this injection of either vehicle (saline) or respective p38α MAPK inhibitor, each respective mouse had its core body temperature recorded once every 10 min for a total of 80 min using a BAT-12 thermometer (Physitemp, Stoelting). Immediately preceding the third temperature reading, mice were administered 8-OH-DPAT (0.1 mg/kg, subcutaneously, 0.1 mL/10 g body weight). Body temperature was recorded for 1 h posttreatment with 8-OH-DPAT, with recordings conducted every 10 min. This experimental design allowed for us to also determine whether MW108 or MW150 exhibited any effects on body temperature on its own in addition to determine whether MW108 or MW150 administration results in a normalization of 5-HT_{1A} receptor sensitivity in SERT Ala56 mice.

HPLC Analysis of Monoamine Levels. Before assessment of monoamine levels, male, SERT Ala56 mice and their SERT Gly56 littermate counterparts were administered either saline (0.1 mL/10 g body weight, intraperitoneally, QD × 7 d), MW108 (10 mg/kg, i.p., QD × 7 d), or MW150 (5 mg/kg, i.p., QD × 7 d) before sample collection. Samples were collected by rapid decapitation. Brain regions were isolated and flash-frozen in liquid nitrogen. Biogenic amine levels were detected utilizing HPLC through the Vanderbilt Molecular Neuroscience core facility, as previously described (37). Biogenic amines were eluted with a mobile phase consisting of 89.5% 0.1 M TCA, 10^{-2} M sodium acetate, 10^{-4} M EDTA, and 10.5% (vol/vol) methanol (pH 3.8). Concentrations were determined using comparisons to injections with known standards.

Western Blotting. Male SERT Ala56 mice and their SERT Gly56 littermate counterparts were treated with either saline (0.1 mL/10 g body weight, intraperitoneally, QD × 7 d), MW108 (10 mg/kg, i.p., QD × 7 d), or MW150 (5 mg/kg, i.p., QD × 7 d) for 1 wk before sample collection. Midbrain samples isolated from these mice after rapid decapitation were flash-frozen in liquid nitrogen and stored at −80 °C until use. Midbrain samples were subsequently homogenized in 350 μL of RIPA buffer (50 mM Tris, pH 7.4, 150 mM NaCl, 1 mM EDTA, 1% Triton X-100, 1% sodium deoxycholate, 0.1% SDS) that contained protease inhibitors (1:100; Sigma Aldrich). Samples were solubilized for 1 h at 4 °C and protein lysates were centrifuged at 4 °C for 10 min at 15,000 × *g* to remove insoluble material. Protein concentrations were determined using the BCA method (ThermoFisher) and 40 μg of total protein was separated by 10% SDS/PAGE and then transferred to PVDF using a semidry transfer unit (Bio-Rad). Membranes were blocked using 5% dry milk in PBS-T for 2 h at room temperature. Membranes were incubated with primary SERT antibody (#HTT-GP-Af1400; Frontier Institute; 1:2,000 for Western blots) overnight at 4 °C. Immunoreactive bands were identified by chemiluminescence (Western Lightning ECL Pro; Perkin-Elmer) and imaged with ImageQuantTM LAS400 (GE Healthcare Life Sciences). SERT expression was normalized to β-actin and analysis was conducted utilizing ImageJ software.

In Vivo Chronoamperometry. Hippocampal clearance of 5-HT mediated by SERT was measure through the use of in vivo chronoamperometry in a manner as previously described (37, 51). Male SERT Ala56 mice and their respective SERT Gly56 littermates were anesthetized using a combination of chloralose (35 mg/kg) and urethane (350 mg/kg). While under anesthesia, each animal underwent endotracheal intubation and a small trachea tube was utilized to aid in breathing for the duration of the procedure. Each animal was subsequently placed into a stereotaxic frame (Kopf Instruments), and an in vivo electrochemical recording assembly was lowered in the CA3 region of the dorsal hippocampus (anterior-posterior, −1.94; medial-lateral, +2.0; dorsal-ventral, −2.0). In vivo electrochemical recording assemblies consisted of a single, carbon fiber electrode (Center for Microelectrode Technology) that had previously undergone five coatings with Nafion and were attached to a seven-barrel micropipette such that the tips were separated by ∼200 μM. Micropipette barrels were filled with 5-HT (200 μM, Sigma Aldrich) dissolved in PBS, pH 7.4. Exogenous 5-HT was applied by pressure injection in volumes ranging from (5–75 nL) to produce signal amplitudes ranging from (0.4–4.32 μM) in randomized order for each respective subject. All high-speed chronoamperometric recordings were made using the FAST-12 system (Quanteon). Oxidation potentials consisted of 100-ms pulses of +0.55 V separated by a 900-ms interval of 0.0 V. An Ag/AgCl reference electrode was placed under the skin behind the skull of each respective subject. Oxidation and reduction currents were digitally integrated during the last 80 ms of each 100-ms voltage pulse. Each Nafion-coated electrode was individually pretested and calibrated for selectivity ratio of 5-HT over 5HIAA greater than 500:1. For data analysis purposes, the oxidation current was converted to micromolar units of 5-HT concentration through the utilization of calibration values determined for each respective electrode in vitro. Clearance rate (T_c), where clearance rate is defined as the slope of the decay curve from 20 to 60% of maximal signal amplitude (most linear portion of the decay), was plotted against maximal signal amplitude (micromolar). Each point on the curves was derived from at least five distinct mice ($n = 5$ per group).

In Vitro Radiolabeled 5-HT Uptake Assay. In vitro 5-HT uptake assays were conducted similarly to those previously described (32). Briefly, SK-N-MC cells stably expressing human SERT (hSERT), a generous gift from H. E. Melikian, University of Massachusetts Medical School, Worchester, MA, were plated at 25,000 cells per well in 12-well plates and were allowed to grow for 48 h before all uptake assays. All uptake assays were conducted in an uptake buffer solution (150 mM NaCl, 10 mM Hepes, 1.8 g/L glucose, 100 μM Ascorbic Acid and 100 μM Pargyline). Anisomycin (Sigma Aldrich) was initially dissolved in DMSO and then further diluted in uptake buffer. Pretreatments consisted of 15-min incubations at 37 °C before 10-min uptake assays at 37 °C utilizing a final concentration of 20 nM [^{3}H]5-HT. To calculate nonspecific uptake, 10 μM paroxetine was utilized to block SERT-mediated [^{3}H]5-HT uptake. After 10-min incubation with 20 nM [^{3}H]5-HT at 37 °C, buffer was aspirated, and cells were washed three times with ice-cold uptake buffer. Cells were solubilized with 0.4 mL Microscint 20 (Packard Bioscience). Accumulated [^{3}H]5-HT was quantified using a TopCount plate scintillation counter (Packard Bioscience). Specific 5-HT uptake was determined by subtracting the amount of [^{3}H]5-HT from samples containing 10 μM paroxetine as described above.

CMMC Patterns Measured in Vitro. SERT Ala56 mice and their SERT Gly56 littermate counterparts underwent repeated administration of either vehicle (saline) or MW150, as described above. After killing, the entire colon was dissected out of each mouse (n = 10–12 mice per group) and cleared of stool pellets with Krebs' solution. The colon was then mounted in an organ bath, which allowed the luminal and serosal superfusion with 35 °C oxygenated Krebs' solution. The height of a reservoir connected to the oral cannula was adjusted to maintain intraluminal pressure at +2 cm. The anal cannula provided a maximum of 2 cm H_2O back pressure. Contractions were imaged with a Logitech Quickcam pro camera positioned 7–8 cm above the colon. Four 15-min videos were captured after a 30-min period of equilibration. Spatiotemporal maps of the diameter at each point along the proximo-distal length of the colon were constructed (122, 123) and used to quantify CMMC frequency, velocity, and length of propagation (43).

Generation of SERT Ala56:p38α MAPK$^{loxP/loxP}$::ePet1 Cre Mice. Mice were generated by crossing 129s4/s6 SERT Ala56 mice (37) to C57BL/6J p38α MAPK$^{loxP/loxP}$::ePet1 Cre mice (33) to obtain SERT Ala56$^{+/-}$:p38α MAPK$^{loxP/WT}$::ePet1 Cre males. SERT Ala56$^{+/-}$:p38α MAPK$^{loxP/WT}$::ePet1 Cre males were bred to SERT Ala56$^{+/-}$:p38α MAPK$^{loxP/WT}$ females to obtain SERT Ala56$^{+/+}$:p38α MAPK$^{loxP/loxP}$::ePet1 Cre (Ala56 p38α^{5HT-}) and SERT Ala56$^{+/+}$:p38α MAPK$^{loxP/loxP}$ (Ala56 p38α^{5HT+}) offspring. Breeding of SERT Ala56 p38α^{5HT-} males and SERT Ala56 p38α^{5HT+} females yielded cohorts utilized for all biochemistry and behavioral studies.

Immunohistochemistry. SERT Ala56 p38α^{5HT-} and SERT Ala56 p38α^{5HT+} male littermates used for immunohistochemistry were anesthetized by intraperitoneal pentobarbital injection (65 mg/kg), and subjected to intracardiac perfusion with cold PBS (pH 7.4) followed by 4% freshly prepared paraformaldehyde (PFA). The remainder of the immunohistochemistry protocol was similar to that previously described (33). Brains were immediately removed, postfixed in PFA at 4 °C overnight, and then cryoprotected in 30% sucrose. Brains were then frozen and sectioned (30 μm) using a sliding microtome (Leica SM-2010R). Free-floating sections were washed 3× in PBS buffer and blocked in PBS buffer containing 0.2% Triton-X and 3% normal donkey serum for 1 h at room temperature. The sections were incubated with primary antibodies (#2079 goat anti–5-HT; Immunostar and #9218 rabbit anti-p38α MAPK; Cell Signaling Technology) overnight at 4 °C followed by fluorophore-conjugated secondary antibodies (2 h, room temperature). DAPI staining and mounting was conducted utilizing Prolong Gold Antifade Reagent with DAPI (ThermoFisher Scientific). Images were obtained utilizing a Nikon A1R confocal contained within the Florida Atlantic University Brain Institute Nikon Center for Excellence.

Statistics. All statistical analyses were conducted utilizing Graphpad Prism 7. One-way or two-way ANOVA, followed by post hoc Tukey's, Bonferroni's, Fisher's, or Sidak's multiple comparison tests were utilized where applicable. Two-way repeated-measures ANOVA, followed by post hoc Bonferroni's multiple comparison tests were utilized to analyze data stemming from 8-OH-DPAT–induced hypothermia assays. McNemar's tests or χ^2 analyses with Yates correction were utilized where applicable for paired control or treatment group comparisons in all tube tests for social-dominance experiments.

Study Approval. All experiments conducted using animal subjects were conducted according to the National Institutes of Health *Guide for the Care and Use of Laboratory Animals* (124). All experiments involving animal subjects were conducted as preapproved by the Vanderbilt University, Columbia University Medical Center and Florida Atlantic University Institutional Animal Care and Use Committees. Male SERT Ala56 mice and their SERT Gly56 male counterparts were generated using heterozygous breeding pairs in a manner described previously (37). Mice utilized for current studies were weaned at 21 d of age, separated by sex, and housed in cages of three to five mixed-genotype littermates per cage. All mice utilized for studies contained herein were between 8 and 16 wk of age and were age-matched to generate cohorts of animals varying by no more than 4 wk of age. All

animals were randomized and coded and all experimenters were blinded to genotype until after all experiments were completed.

ACKNOWLEDGMENTS. The authors thank Haley E. Melikian (University of Massachusetts Medical School) for the generous gift of SK-N-MC cells stably expressing human serotonin transporter; and Tracy Moore-Jarrett, Jane Wright, Chris Svitek, Catherine Nettesheim, and Matthew Gross for excellent technical support. Funding for these studies was generously provided by the Simon's Foundation (R.D.B.); NIH Grants MH096972 (to R.D.B.), MH094527 (to R.D.B.), NS007491 (to M.J.R.), NS015547 (to M.D.G.), DK093786 (to K.G.M.), and U01AG043415 (to D.M.W.); the PhRMA Foundation (M.J.R.); and the Brain and Behavior Research Foundation (M.J.R.).

1. Robinson EB, Neale BM, Hyman SE (2015) Genetic research in autism spectrum disorders. *Curr Opin Pediatr* 27:685–691.
2. Weiner DJ, et al.; iPSYCH-Broad Autism Group; Psychiatric Genomics Consortium Autism Group (2017) Polygenic transmission disequilibrium confirms that common and rare variation act additively to create risk for autism spectrum disorders. *Nat Genet* 49:978–985.
3. American Psychiatric Association (2013) *Diagnostic and Statistical Manual of Mental Disorders* (American Psychiatric Association, Washington, DC), 5th Ed.
4. Developmental Disabilities Monitoring Network Surveillance Year 2010 Principal Investigators; Centers for Disease Control and Prevention (CDC) (2014) Prevalence of autism spectrum disorder among children aged 8 years—Autism and developmental disabilities monitoring network, 11 sites, United States, 2010. *MMWR Surveill Summ* 63:1–21.
5. Baio J, et al. (2018) Prevalence of autism spectrum disorder among children aged 8 years—Autism and developmental disabilities monitoring network, 11 sites, United States, 2014. *MMWR Surveill Summ* 67:1–23.
6. Buescher AV, Cidav Z, Knapp M, Mandell DS (2014) Costs of autism spectrum disorders in the United Kingdom and the United States. *JAMA Pediatr* 168:721–728.
7. Leigh JP, Du J (2015) Brief report: Forecasting the economic burden of autism in 2015 and 2025 in the United States. *J Autism Dev Disord* 45:4135–4139.
8. Politte LC, McDougle CJ (2014) Atypical antipsychotics in the treatment of children and adolescents with pervasive developmental disorders. *Psychopharmacology (Berl)* 231:1023–1036.
9. Ghosh A, Michalon A, Lindemann L, Fontoura P, Santarelli L (2013) Drug discovery for autism spectrum disorder: Challenges and opportunities. *Nat Rev Drug Discov* 12: 777–790.
10. Veenstra-VanderWeele J, Blakely RD (2012) Networking in autism: Leveraging genetic, biomarker and model system findings in the search for new treatments. *Neuropsychopharmacology* 37:196–212.
11. Cook EH, Jr, et al. (1993) Platelet serotonin studies in hyperserotonemic relatives of children with autistic disorder. *Life Sci* 52:2005–2015.
12. Schain RJ, Freedman DX (1961) Studies on 5-hydroxyindole metabolism in autistic and other mentally retarded children. *J Pediatr* 58:315–320.
13. Hanley HG, Stahl SM, Freedman DX (1977) Hyperserotonemia and amine metabolites in autistic and retarded children. *Arch Gen Psychiatry* 34:521–531.
14. Mulder EJ, et al. (2004) Platelet serotonin levels in pervasive developmental disorders and mental retardation: Diagnostic group differences, within-group distribution, and behavioral correlates. *J Am Acad Child Adolesc Psychiatry* 43:491–499.
15. Abney M, McPeek MS, Ober C (2001) Broad and narrow heritabilities of quantitative traits in a founder population. *Am J Hum Genet* 68:1302–1307.
16. Sandin S, et al. (2014) The familial risk of autism. *JAMA* 311:1770–1777.
17. Cross S, et al. (2008) Molecular genetics of the platelet serotonin system in first-degree relatives of patients with autism. *Neuropsychopharmacology* 33:353–360.
18. Brindley RL, Bauer MB, Blakely RD, Currie KPM (2016) An interplay between the serotonin transporter (SERT) and 5-HT receptors controls stimulus-secretion coupling in sympathoadrenal chromaffin cells. *Neuropharmacology* 110:438–448.
19. Wu HH, Choi S, Levitt P (2016) Differential patterning of genes involved in serotonin metabolism and transport in extra-embryonic tissues of the mouse. *Placenta* 42: 74–83.
20. Chen JX, Pan H, Rothman TP, Wade PR, Gershon MD (1998) Guinea pig 5-HT transporter: Cloning, expression, distribution, and function in intestinal sensory reception. *Am J Physiol* 275:G433–G448.
21. Chen JJ, et al. (2001) Maintenance of serotonin in the intestinal mucosa and ganglia of mice that lack the high-affinity serotonin transporter: Abnormal intestinal motility and the expression of cation transporters. *J Neurosci* 21:6348–6361.
22. Wade PR, et al. (1996) Localization and function of a 5-HT transporter in crypt epithelia of the gastrointestinal tract. *J Neurosci* 16:2352–2364.
23. Kristensen AS, et al. (2011) SLC6 neurotransmitter transporters: Structure, function, and regulation. *Pharmacol Rev* 63:585–640.
24. Sutcliffe JS, et al. (2005) Allelic heterogeneity at the serotonin transporter locus (SLC6A4) confers susceptibility to autism and rigid-compulsive behaviors. *Am J Hum Genet* 77:265–279.
25. Canli T, Lesch KP (2007) Long story short: The serotonin transporter in emotion regulation and social cognition. *Nat Neurosci* 10:1103–1109.
26. Coates MD, et al. (2004) Molecular defects in mucosal serotonin content and decreased serotonin reuptake transporter in ulcerative colitis and irritable bowel syndrome. *Gastroenterology* 126:1657–1664.
27. Blakely RD, et al. (1998) Regulated phosphorylation and trafficking of antidepressant-sensitive serotonin transporter proteins. *Biol Psychiatry* 44:169–178.
28. Steiner JA, Carneiro AM, Blakely RD (2008) Going with the flow: Trafficking-dependent and -independent regulation of serotonin transport. *Traffic* 9:1393–1402.
29. McCauley JL, et al. (2004) Linkage and association analysis at the serotonin transporter (SLC6A4) locus in a rigid-compulsive subset of autism. *Am J Med Genet B Neuropsychiatr Genet* 127B:104–112.
30. Prasad HC, Steiner JA, Sutcliffe JS, Blakely RD (2009) Enhanced activity of human serotonin transporter variants associated with autism. *Philos Trans R Soc Lond B Biol Sci* 364:163–173.
31. Prasad HC, et al. (2005) Human serotonin transporter variants display altered sensitivity to protein kinase G and p38 mitogen-activated protein kinase. *Proc Natl Acad Sci USA* 102:11545–11550.
32. Zhu CB, Blakely RD, Hewlett WA (2006) The proinflammatory cytokines interleukin-1beta and tumor necrosis factor-alpha activate serotonin transporters. *Neuropsychopharmacology* 31:2121–2131.
33. Baganz NL, et al. (2015) A requirement of serotonergic p38α mitogen-activated protein kinase for peripheral immune system activation of CNS serotonin uptake and serotonin-linked behaviors. *Transl Psychiatry* 5:e671.
34. Zhu CB, et al. (2010) Interleukin-1 receptor activation by systemic lipopolysaccharide induces behavioral despair linked to MAPK regulation of CNS serotonin transporters. *Neuropsychopharmacology* 35:2510–2520.
35. Garbett K, et al. (2008) Immune transcriptome alterations in the temporal cortex of subjects with autism. *Neurobiol Dis* 30:303–311.
36. Veenstra-Vanderweele J, et al. (2009) Modeling rare gene variation to gain insight into the oldest biomarker in autism: Construction of the serotonin transporter Gly56Ala knock-in mouse. *J Neurodev Disord* 1:158–171.
37. Veenstra-VanderWeele J, et al. (2012) Autism gene variant causes hyperserotonemia, serotonin receptor hypersensitivity, social impairment and repetitive behavior. *Proc Natl Acad Sci USA* 109:5469–5474.
38. Kerr TM, et al. (2013) Genetic background modulates phenotypes of serotonin transporter Ala56 knock-in mice. *Mol Autism* 4:35.
39. Siemann JK, et al. (2017) An autism-associated serotonin transporter variant disrupts multisensory processing. *Transl Psychiatry* 7:e1067.
40. Baum SH, Stevenson RA, Wallace MT (2015) Behavioral, perceptual, and neural alterations in sensory and multisensory function in autism spectrum disorder. *Prog Neurobiol* 134:140–160.
41. Marler S, et al. (2017) Association of rigid-compulsive behavior with functional constipation in autism spectrum disorder. *J Autism Dev Disord* 47:1673–1681.
42. Marler S, et al. (2016) Brief report: Whole blood serotonin levels and gastrointestinal symptoms in autism spectrum disorder. *J Autism Dev Disord* 46:1124–1130.
43. Margolis KG, et al. (2016) Serotonin transporter variant drives preventable gastrointestinal abnormalities in development and function. *J Clin Invest* 126:2221–2235.
44. Watterson DM, et al. (2013) Development of novel in vivo chemical probes to address CNS protein kinase involvement in synaptic dysfunction. *PLoS One* 8:e66226.
45. Zhou Z, et al. (2017) Retention of normal glia function by an isoform-selective protein kinase inhibitor drug candidate that modulates cytokine production and cognitive outcomes. *J Neuroinflammation* 14:75.
46. Arthur JS, Ley SC (2013) Mitogen-activated protein kinases in innate immunity. *Nat Rev Immunol* 13:679–692.
47. Bachstetter AD, Watterson DM, Van Eldik LJ (2014) Target engagement analysis and link to pharmacodynamic endpoint for a novel class of CNS-penetrant and efficacious p38α MAPK inhibitors. *J Neuroimmune Pharmacol* 9:454–460.
48. Munoz L, et al. (2007) A novel p38 alpha MAPK inhibitor suppresses brain proinflammatory cytokine up-regulation and attenuates synaptic dysfunction and behavioral deficits in an Alzheimer's disease mouse model. *J Neuroinflammation* 4:21.
49. Zhu CB, Carneiro AM, Dostmann WR, Hewlett WA, Blakely RD (2005) p38 MAPK activation elevates serotonin transport activity via a trafficking-independent, protein phosphatase 2A-dependent process. *J Biol Chem* 280:15649–15658.
50. Samuvel DJ, Jayanthi LD, Bhat NR, Ramamoorthy S (2005) A role for p38 mitogen-activated protein kinase in the regulation of the serotonin transporter: Evidence for distinct cellular mechanisms involved in transporter surface expression. *J Neurosci* 25: 29–41.
51. Daws LC, Toney GM, Davis DJ, Gerhardt GA, Frazer A (1997) In vivo chronoamperometric measurements of the clearance of exogenously applied serotonin in the rat dentate gyrus. *J Neurosci Methods* 78:139–150.
52. Canal CE, et al. (2010) The serotonin 2C receptor potently modulates the head-twitch response in mice induced by a phenethylamine hallucinogen. *Psychopharmacology (Berl)* 209:163–174.
53. Fantegrossi WE, et al. (2010) Interaction of 5-HT2A and 5-HT2C receptors in R(-)-2,5-dimethoxy-4-iodoamphetamine-elicited head twitch behavior in mice. *J Pharmacol Exp Ther* 335:728–734.
54. Canal CE, Morgan D (2012) Head-twitch response in rodents induced by the hallucinogen 2,5-dimethoxy-4-iodoamphetamine: A comprehensive history, a re-evaluation of mechanisms, and its utility as a model. *Drug Test Anal* 4:556–576.
55. Buie T, et al. (2010) Evaluation, diagnosis, and treatment of gastrointestinal disorders in individuals with ASDs: A consensus report. *Pediatrics* 125(Suppl 1):S1–S18.
56. Gorrindo P, et al. (2012) Gastrointestinal dysfunction in autism: Parental report, clinical evaluation, and associated factors. *Autism Res* 5:101–108.
57. Gershon MD (2013) 5-Hydroxytryptamine (serotonin) in the gastrointestinal tract. *Curr Opin Endocrinol Diabetes Obes* 20:14–21.
58. Schroeter S, Levey AI, Blakely RD (1997) Polarized expression of the antidepressant-sensitive serotonin transporter in epinephrine-synthesizing chromaffin cells of the rat adrenal gland. *Mol Cell Neurosci* 9:170–184.

59. Mortensen OV, Kristensen AS, Rudnick G, Wiborg O (1999) Molecular cloning, expression and characterization of a bovine serotonin transporter. *Brain Res Mol Brain Res* 71:120–126.
60. Almaça J, et al. (2016) Human beta cells produce and release serotonin to inhibit glucagon secretion from alpha cells. *Cell Rep* 17:3281–3291.
61. Romay-Tallon R, et al. (2017) Comparative study of two protocols for quantitative image-analysis of serotonin transporter clustering in lymphocytes, a putative biomarker of therapeutic efficacy in major depression. *Biomark Res* 5:27.
62. Rivera-Baltanas T, et al. (2015) Serotonin transporter clustering in blood lymphocytes predicts the outcome on anhedonia scores in naïve depressive patients treated with antidepressant medication. *Ann Gen Psychiatry* 14:45.
63. Scott MM, et al. (2005) A genetic approach to access serotonin neurons for in vivo and in vitro studies. *Proc Natl Acad Sci USA* 102:16472–16477.
64. Scott MM, Krueger KC, Deneris ES (2005) A differentially autoregulated Pet-1 enhancer region is a critical target of the transcriptional cascade that governs serotonin neuron development. *J Neurosci* 25:2628–2636.
65. Ramamoorthy S, Samuvel DJ, Buck ER, Rudnick G, Jayanthi LD (2007) Phosphorylation of threonine residue 276 is required for acute regulation of serotonin transporter by cyclic GMP. *J Biol Chem* 282:11639–11647.
66. Wang F, Kessels HW, Hu H (2014) The mouse that roared: Neural mechanisms of social hierarchy. *Trends Neurosci* 37:674–682.
67. Kunkel T, Wang H (2018) Socially dominant mice in C57BL6 background show increased social motivation. *Behav Brain Res* 336:173–176.
68. Spencer CM, Alekseyenko O, Serysheva E, Yuva-Paylor LA, Paylor R (2005) Altered anxiety-related and social behaviors in the Fmr1 knockout mouse model of fragile X syndrome. *Genes Brain Behav* 4:420–430.
69. Margolis KG (2017) A role for the serotonin reuptake transporter in the brain and intestinal features of autism spectrum disorders and developmental antidepressant exposure. *J Chem Neuroanat* 83-84:36–40.
70. Muller CL, Anacker AMJ, Veenstra-VanderWeele J (2016) The serotonin system in autism spectrum disorder: From biomarker to animal models. *Neuroscience* 321:24–41.
71. Chen R, et al. (2017) Leveraging blood serotonin as an endophenotype to identify de novo and rare variants involved in autism. *Mol Autism* 8:14.
72. Chugani DC (2002) Role of altered brain serotonin mechanisms in autism. *Mol Psychiatry* 7(Suppl 2):S16–S17.
73. Chugani DC, et al. (1997) Altered serotonin synthesis in the dentatothalamocortical pathway in autistic boys. *Ann Neurol* 42:666–669.
74. Chugani DC, et al. (1999) Developmental changes in brain serotonin synthesis capacity in autistic and nonautistic children. *Ann Neurol* 45:287–295.
75. Dohn MR, et al. (2017) The gain-of-function integrin β3 Pro33 variant alters the serotonin system in the mouse brain. *J Neurosci* 37:11271–11284.
76. Weiss LA, Ober C, Cook EH, Jr (2006) ITGB3 shows genetic and expression interaction with SLC6A4. *Hum Genet* 120:93–100.
77. Napolioni V, et al. (2011) Family-based association study of ITGB3 in autism spectrum disorder and its endophenotypes. *Eur J Hum Genet* 19:353–359.
78. Ma DQ, et al. (2010) Association and gene-gene interaction of SLC6A4 and ITGB3 in autism. *Am J Med Genet B Neuropsychiatr Genet* 153B:477–483.
79. Coutinho AM, et al. (2007) Evidence for epistasis between SLC6A4 and ITGB3 in autism etiology and in the determination of platelet serotonin levels. *Hum Genet* 121:243–256.
80. McDougle CJ, et al. (1996) Effects of tryptophan depletion in drug-free adults with autistic disorder. *Arch Gen Psychiatry* 53:993–1000.
81. Zhang WQ, et al. (2015) Acute dietary tryptophan manipulation differentially alters social behavior, brain serotonin and plasma corticosterone in three inbred mouse strains. *Neuropharmacology* 90:1–8.
82. Williams K, Brignell A, Randall M, Silove N, Hazell P (2013) Selective serotonin reuptake inhibitors (SSRIs) for autism spectrum disorders (ASD). *Cochrane Database Syst Rev,* CD004677.
83. Ji N, Findling RL (2015) An update on pharmacotherapy for autism spectrum disorder in children and adolescents. *Curr Opin Psychiatry* 28:91–101.
84. Hollander E, et al. (2012) A double-blind placebo-controlled trial of fluoxetine for repetitive behaviors and global severity in adult autism spectrum disorders. *Am J Psychiatry* 169:292–299.
85. McDougle CJ, et al. (1996) A double-blind, placebo-controlled study of fluvoxamine in adults with autistic disorder. *Arch Gen Psychiatry* 53:1001–1008.
86. Costa L, Sardone LM, Lacivita E, Leopoldo M, Ciranna L (2015) Novel agonists for serotonin 5-HT7 receptors reverse metabotropic glutamate receptor-mediated long-term depression in the hippocampus of wild-type and Fmr1 KO mice, a model of fragile X syndrome. *Front Behav Neurosci* 9:65.
87. Lim CS, et al. (2014) Pharmacological rescue of Ras signaling, GluA1-dependent synaptic plasticity, and learning deficits in a fragile X model. *Genes Dev* 28:273–289.
88. Costa L, et al. (2012) Activation of 5-HT7 serotonin receptors reverses metabotropic glutamate receptor-mediated synaptic plasticity in wild-type and Fmr1 knockout mice, a model of fragile X syndrome. *Biol Psychiatry* 72:924–933.
89. Hanson AC, Hagerman RJ (2014) Serotonin dysregulation in fragile X syndrome: Implications for treatment. *Intractable Rare Dis Res* 3:110–117.
90. Greiss Hess L, et al. (2016) A randomized, double-blind, placebo-controlled trial of low-dose sertraline in young children with fragile X syndrome. *J Dev Behav Pediatr* 37:619–628.
91. Berry-Kravis E, Potanos K (2004) Psychopharmacology in fragile X syndrome—Present and future. *Ment Retard Dev Disabil Res Rev* 10:42–48.
92. Nakai N, et al. (2017) Serotonin rebalances cortical tuning and behavior linked to autism symptoms in 15q11-13 CNV mice. *Sci Adv* 3:e1603001.
93. Panzini CM, Ehlinger DG, Alchahin AM, Guo Y, Commons KG (2017) 16p11.2 deletion syndrome mice perseverate with active coping response to acute stress—Rescue by blocking 5-HT2A receptors. *J Neurochem* 143:708–721.
94. Walsh JJ, et al. (2018) 5-HT release in nucleus accumbens rescues social deficits in mouse autism model. *Nature* 560:589–594.
95. Guo YP, Commons KG (2017) Serotonin neuron abnormalities in the BTBR mouse model of autism. *Autism Res* 10:66–77.
96. McFarlane HG, et al. (2008) Autism-like behavioral phenotypes in BTBR T+tf/J mice. *Genes Brain Behav* 7:152–163.
97. Meyza KZ, Blanchard DC (2017) The BTBR mouse model of idiopathic autism—Current view on mechanisms. *Neurosci Biobehav Rev* 76:99–110.
98. Pearson BL, et al. (2012) Absence of social conditioned place preference in BTBR T+ tf/J mice: Relevance for social motivation testing in rodent models of autism. *Behav Brain Res* 233:99–104.
99. Gould GG, et al. (2011) Density and function of central serotonin (5-HT) transporters, 5-HT1A and 5-HT2A receptors, and effects of their targeting on BTBR T+tf/J mouse social behavior. *J Neurochem* 116:291–303.
100. Amodeo DA, Rivera E, Cook EH, Jr, Sweeney JA, Ragozzino ME (2017) $5HT_{2A}$ receptor blockade in dorsomedial striatum reduces repetitive behaviors in BTBR mice. *Genes Brain Behav* 16:342–351.
101. Holloway T, et al. (2013) Prenatal stress induces schizophrenia-like alterations of serotonin 2A and metabotropic glutamate 2 receptors in the adult offspring: Role of maternal immune system. *J Neurosci* 33:1088–1098.
102. Kopec AM, Fiorentino MR, Bilbo SD (2018) Gut-immune-brain dysfunction in autism: Importance of sex. *Brain Res* 1693:214–217.
103. Goodwin MS, Cowen MA, Goodwin TC (1971) Malabsorption and cerebral dysfunction: A multivariate and comparative study of autistic children. *J Autism Child Schizophr* 1:48–62.
104. Peters B, et al. (2014) Rigid-compulsive behaviors are associated with mixed bowel symptoms in autism spectrum disorder. *J Autism Dev Disord* 44:1425–1432.
105. Kendig DM, Grider JR (2015) Serotonin and colonic motility. *Neurogastroenterol Motil* 27:899–905.
106. Li Z, et al. (2011) Essential roles of enteric neuronal serotonin in gastrointestinal motility and the development/survival of enteric dopaminergic neurons. *J Neurosci* 31:8998–9009.
107. Kulkarni S, et al. (2017) Adult enteric nervous system in health is maintained by a dynamic balance between neuronal apoptosis and neurogenesis. *Proc Natl Acad Sci USA* 114:E3709–E3718.
108. Liu MT, Kuan YH, Wang J, Hen R, Gershon MD (2009) 5-HT4 receptor-mediated neuroprotection and neurogenesis in the enteric nervous system of adult mice. *J Neurosci* 29:9683–9699.
109. Turner RC, et al. (2013) Modeling clinically relevant blast parameters based on scaling principles produces functional & histological deficits in rats. *Exp Neurol* 248: 520–529.
110. Masi A, et al. (2015) Cytokine aberrations in autism spectrum disorder: A systematic review and meta-analysis. *Mol Psychiatry* 20:440–446.
111. Molloy CA, et al. (2006) Elevated cytokine levels in children with autism spectrum disorder. *J Neuroimmunol* 172:198–205.
112. Napolioni V, et al. (2013) Plasma cytokine profiling in sibling pairs discordant for autism spectrum disorder. *J Neuroinflammation* 10:38.
113. Onore CE, et al. (2013) Inflammatory macrophage phenotype in BTBR T+tf/J mice. *Front Neurosci* 7:158.
114. Onore CE, Schwartzer JJ, Careaga M, Berman RF, Ashwood P (2014) Maternal immune activation leads to activated inflammatory macrophages in offspring. *Brain Behav Immun* 38:220–226.
115. Arrode-Brusés G, Brusés JL (2012) Maternal immune activation by poly I:C induces expression of cytokines IL-1β and IL-13, chemokine MCP-1 and colony stimulating factor VEGF in fetal mouse brain. *J Neuroinflammation* 9:83.
116. Kirsten TB, Lippi LL, Bevilacqua E, Bernardi MM (2013) LPS exposure increases maternal corticosterone levels, causes placental injury and increases IL-1B levels in adult rat offspring: Relevance to autism. *PLoS One* 8:e82244.
117. Hsiao EY, McBride SW, Chow J, Mazmanian SK, Patterson PH (2012) Modeling an autism risk factor in mice leads to permanent immune dysregulation. *Proc Natl Acad Sci USA* 109:12776–12781.
118. Xing B, Bachstetter AD, Van Eldik LJ (2015) Inhibition of neuronal p38α, but not p38β MAPK, provides neuroprotection against three different neurotoxic insults. *J Mol Neurosci* 55:509–518.
119. Roy SM, et al. (2015) Targeting human central nervous system protein kinases: An isoform selective p38αMAPK inhibitor that attenuates disease progression in Alzheimer's disease mouse models. *ACS Chem Neurosci* 6:666–680.
120. Bachstetter AD, et al. (2011) Microglial p38α MAPK is a key regulator of proinflammatory cytokine up-regulation induced by toll-like receptor (TLR) ligands or beta-amyloid (Aβ). *J Neuroinflammation* 8:79.
121. Rutigliano G, Stazi M, Arancio O, Watterson DM, Origlia N (2018) An isoform-selective p38α mitogen-activated protein kinase inhibitor rescues early entorhinal cortex dysfunctions in a mouse model of Alzheimer's disease. *Neurobiol Aging* 70:86–91.
122. Welch MG, Margolis KG, Li Z, Gershon MD (2014) Oxytocin regulates gastrointestinal motility, inflammation, macromolecular permeability, and mucosal maintenance in mice. *Am J Physiol Gastrointest Liver Physiol* 307:G848–G862.
123. Gwynne RM, Thomas EA, Goh SM, Sjövall H, Bornstein JC (2004) Segmentation induced by intraluminal fatty acid in isolated guinea-pig duodenum and jejunum. *J Physiol* 556:557–569.
124. National Research Council of the National Academies (2011) *Guide for the Care and Use of Laboratory Animals* (The National Academies Press, Washington, DC), 8th Ed.